Ab initio calculations of the optical properties of crystalline and liquid InSb

Haruyuki Sano[1,a] and Goro Mizutani[2]
[1]*National Institute of Technology, Ishikawa College, Kitacyujo, Tsubata, Ishikawa 929-0392, Japan*
[2]*School of Materials Science, Japan Advanced Institute of Science and Technology, Tatsunokuchi, Ishikawa 923-1292, Japan*

(Received 21 July 2015; accepted 28 October 2015; published online 4 November 2015)

Ab initio calculations of the electronic and optical properties of InSb were performed for both the crystalline and liquid states. Two sets of atomic structure models for liquid InSb at 900 K were obtained by ab initio molecular dynamics simulations. To reduce the effect of structural peculiarities in the liquid models, an averaging of the two sets of the calculated electronic and optical properties corresponding to the two liquid models was performed. The calculated results indicate that, owing to the phase transition from crystal to liquid, the density of states around the Fermi level increases. As a result, the energy band gap opening near the Fermi level disappears. Consequently, the optical properties change from semiconductor to metallic behavior. Namely, owing to the melting of InSb, the interband transition peaks disappear and a Drude-like dispersion is observed in the optical dielectric functions. The optical absorption at a photon energy of 3.06 eV, which is used in Blu-ray Disc systems, increases owing to the melting of InSb. This increase in optical absorption is proposed to result from the increased optical transitions below 2 eV. [http://dx.doi.org/10.1063/1.4935438]

I. INTRODUCTION

An active layer with optical nonlinearity is the key to the super-resolution readout technology for large capacity optical discs.[1–7] The heat produced by laser light irradiation causes melting of the active layer within a small region. Because of the change in the optical properties arising from the phase transition, the molten region in the active layer behaves like a small aperture[8] or a small mask[9,10] for the light exposure to enable correct read out of the recording pits/marks smaller than the optical diffraction limit. Therefore, a complete understanding of the mechanism of the change in optical properties of the active layer material arising from the melting is required for the development of the super-resolution readout technology.

InSb, a narrow band gap semiconductor in the crystalline state, is the best candidate material for use as the active layer in a super-resolution optical disc.[6,7] The change in the optical properties of InSb during phase transition was experimentally studied for the first time by Kuwahara et al.[11] Their spectroscopic ellipsometry measurements showed that the optical dielectric function in the solid state has several peaks corresponding to interband transitions. Conversely, these peaks disappear in the liquid state and a Drude-like behavior becomes dominant in the dielectric function. Their experimental results also indicate that the optical absorption of InSb increases because of the melting at a wavelength of 405 nm, which is used in Blu-ray Disc systems.[11] In this case, a small mask, corresponding to the molten InSb region, is suggested to be the origin of the super-resolution effect.[9,10]

[a]Author to whom correspondence should be addressed. Electronic mail: h-sano@ishikawa-nct.ac.jp

Although the experimental data on the optical properties of InSb is useful for the analysis of the super-resolution effect,[10] they do not provide sufficient information on the mechanism of the change in optical properties arising from the melting, that is, the change in the electronic states of InSb. Hence, to clarify this mechanism, ab initio calculations of the electronic states and optical properties for both solid and liquid InSb are required. Several ab initio calculations of the electronic states of crystalline[12–15] and amorphous[16,17] InSb have previously been performed. Optical reflectivity[12] and optical dielectric functions[13,14,18] have also been calculated. Conversely, there have only been a few studies on the ab initio calculation of the electronic states of liquid InSb.[19] Gu et al. have reported the electronic structure and optical conductivity of liquid InSb.[19] However, because they expressed the optical conductivity in arbitrary units, their reported value cannot be used for the quantitative comparison of the optical responses between the liquid and crystalline state. To date, there has been no precise calculation of the optical properties, such as optical dielectric functions or refractive indices, for liquid InSb.

In the present study, we have performed ab initio calculations of the electronic states and the optical properties of InSb. Because the same calculation code and similar approximation parameters were used for both crystalline and liquid states, the calculated results can be used to quantitatively compare the differences between both states. Such comparisons are useful for interpreting the changes in the electronic and optical properties that arise from the melting. Note that the approximations used in this ab initio calculation are an improvement to those used in Ref. 19. Some of the results in our current calculation, namely, the total electronic density of states (DOS) and the imaginary part of optical dielectric functions, have been reported in Ref. 20. In the present paper, we present our calculated results on electronic band structures, partial DOS, and refractive indices that are substantiated by a detailed discussion on the changes in the electronic and optical properties arising from the melting.

II. COMPUTATIONAL METHODS

This study was performed using the projector augmented wave method[21,22] including spin–orbit coupling (SOC) effects as implemented in the Vienna Ab initio Simulation Package.[23,24] The generalized gradient approximation (GGA), proposed by the Perdew–Burke–Ernzerhof (PBE) functional,[25] was employed to describe the exchange-correlation potential in the standard density functional theory calculations. When using the GGA or the local-density approximation (LDA), no gap opening in the band structure calculated for narrow band gap semiconductors, such as InSb, were observed. Recently, Kim et al.[15] reported that the modified Becke–Johnson exchange potential combined with the local-density approximation (MBJLDA) method[26] provided accurate gap energy values for InSb at a low computational cost. This MBJLDA method was also used in the present calculations of the electronic states and optical properties. The Brillouin-zone integrations have been performed on Γ-centered k-point meshes using the Gaussian smearing method with a width of 0.1 eV. For the crystalline and liquid states of InSb, $(24 \times 24 \times 24)$ and $(3 \times 3 \times 3)$ k points were used, respectively. Optical dielectric functions (ε) were obtained by calculating the electronic transitions between the valence and conduction band states within the electric dipole approximation.[27] Local field effects and intraband transitions expressed by the Drude-like term in the dielectric function were not considered in this calculation. The complex refractive indices ($\tilde{n} = n + ik$) were obtained using the relation $\tilde{n} = \sqrt{\varepsilon}$.

For the calculation of crystal InSb, a face centered cubic (fcc) crystal structure with the experimental equilibrium lattice constant at 300 K, that is, $a = 0.6479$ nm,[28] was used. The disordered structure of liquid InSb depends on the temperature, that is, the degree of the disorder (the complexity of the structure) becomes larger as the temperature increases. A study of the theoretical simulation of the optical disc including an active layer of InSb[10] indicated that the temperature of molten InSb reached 860–900 K in the super-resolution states at an incident light power of 2.0–2.2 mW. In this study, therefore, we constructed model atomic structures for liquid InSb at a temperature of 900 K by using ab initio molecular dynamics (MD) simulations as follows. A cubic super cell, with a lattice parameter of 1.2956 nm, included 32 In atoms and 32 Sb atoms. The MD calculations were performed within the GGA-PBE approximation, considering no SOC effects

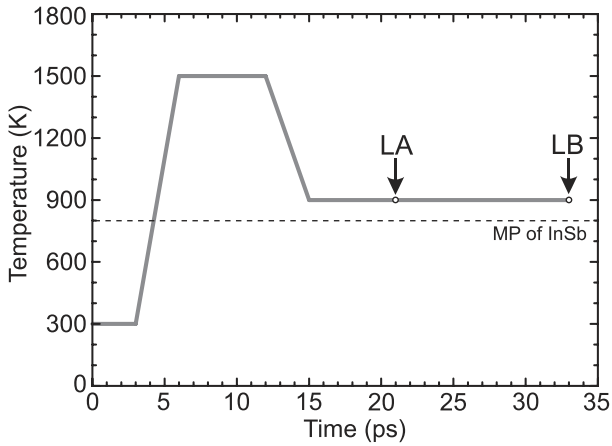

FIG. 1. Temperature control of the MD calculation. The dashed horizontal line denotes the melting point of InSb.

and using only the Γ-point in the Brillouin-zone integration. A canonical ensemble with a Nosé thermostat[29] was used for temperature control, and the time step was set to be 3 fs. As an initial geometry, the crystal structure of InSb was adopted, and the temperature was changed, as shown in Fig. 1. It was confirmed that when the temperature exceeded the melting point of InSb (798 K), the atoms moved around in the cell so that the atomic geometry varied with time. Annealing at 1500 K was conducted to eliminate any trace of crystallinity. After reaching thermodynamic equilibrium at 900 K, we obtained two model atomic structures for liquid InSb as snapshots at two different time points, LA and LB, as shown in Fig. 1. The elapsed time from setting the temperature at 900 K to the time point LA was 6 ps, which is much longer than the time scale of the phonon oscillation of InSb. Thus, it is expected that liquid models in sufficient equilibrium at 900 K can be produced at and after the time point LA. Because the atoms in the liquid states migrated a few nanometers during the elapsed time of 12 ps between LA and LB, these two liquid models, chosen from a series of the MD calculations, have different atomic geometries, as shown in Fig. 2. The calculated electronic states and optical properties for these two model structures are very similar with only small differences. (An example is shown in the next section.) Therefore, these models can be used to discuss the general nature of the electronic and optical properties of liquid InSb because they display no prominent features resulting from structural peculiarities. Furthermore, to eliminate the remaining small effect of the structural peculiarities, we carried out the average operation for the two sets of the calculated electronic and optical properties corresponding to the two liquid models with different structures.

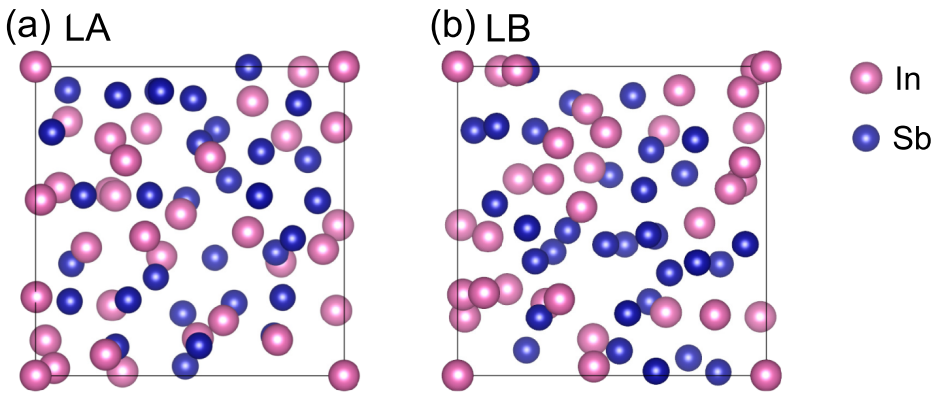

FIG. 2. Model atomic structures of liquid InSb. (a) LA and (b) LB denote snapshots at different time points in the MD calculation at 900 K, as shown in Fig. 1.

In the model of liquid InSb, we adopted the density of the crystalline state (5.78 g/cm^3) that was used by Los et al.[16] in their MD calculation of InSb. The actual density of liquid InSb in the temperature range of 900–1500 K is approximately 5–11% larger than that of the crystalline state.[30] However, this relatively small increase in the density should have only a slight influence on the MD calculation because the MD calculation reported in Ref. 16 provided similar results of the structural properties for the two models at the crystalline density and an approximately 6% larger density.

III. RESULTS AND DISCUSSION

Electronic energy band structures of crystalline InSb, calculated by the GGA-PBE and MBJLDA methods, are shown in Fig. 3(a) and 3(b), respectively. The band structure obtained from the MBJLDA calculation has a small band gap opening at the Γ point near the Fermi level, whereas the GGA-PBE calculation yields no band gap. The band gap energy predicted by the MBJLDA calculation is 0.296 eV. This value is in good agreement with the experimental value of 0.24 eV.[31] Our result, shown in Fig. 3(b), is also consistent with the band structure obtained from a previous MBJLDA calculation.[15] As discussed in Ref. 15, the experimental values of some critical point energies at the X and L points, as well as the Γ point, are well reproduced by the MBJLDA calculation. Thus, it follows that the MBJLDA calculation that takes into consideration the SOC

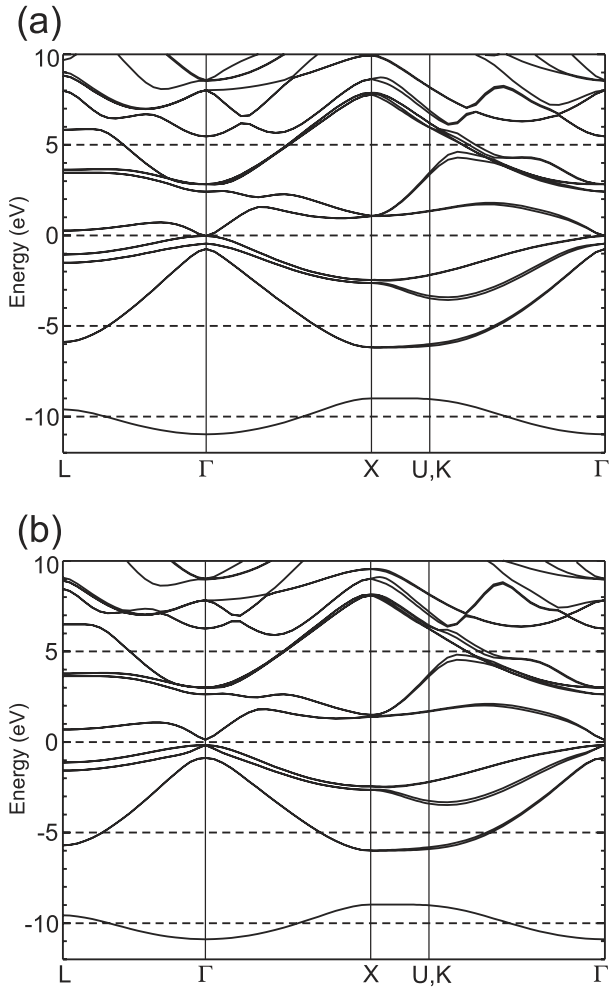

FIG. 3. Electronic energy band structures of crystal InSb along the L-Γ-X-U (K)-Γ path obtained from (a) GGA-PBE and (b) MBJLDA calculations. Spin–orbital coupling (SOC) was considered in the calculations.

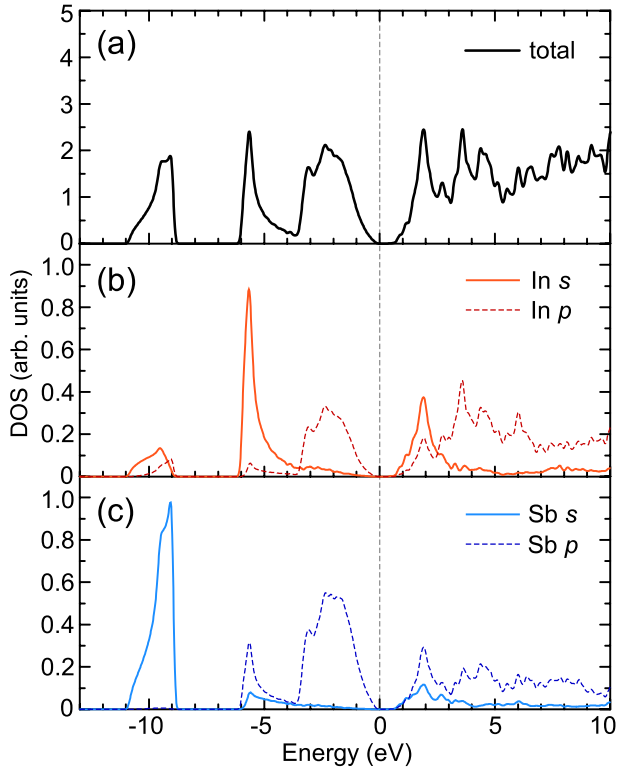

FIG. 4. Electronic density of states (DOS) of crystal InSb. (a) Total DOS. Partial DOS projected onto the molecular orbitals of In (b) and Sb (c).

effects, which is used in this study, can provide valid and accurate results for the electronic states of InSb.

Figure 4 shows the DOS of the InSb crystal obtained by our MBJLDA–SOC calculation. The origin of the bands in crystal InSb is suggested by the analysis of the partial DOS of In and Sb atoms, as shown in Fig. 4(b) and 4(c). Narrow bands at the energies −9.5 and −5.5 eV are attributed to the s-orbitals of Sb and In, respectively. A broad band in the −4 to −1 eV range is attributed to the mixing of the p-orbitals of In and Sb. Figure 5 shows the DOS of liquid InSb obtained by the MBJLDA–SOC calculation. Comparing the DOS of the LA and LB states in Fig. 5(a), it is observed that these have similar envelopes but exhibit minor differences in the fine structure resulting from the structural peculiarities of the LA and LB states. To reduce the effect of these peculiarities, the average of the DOS of the LA and LB states is shown in Fig. 5(b), 5(c) and 5(d). Furthermore, the partial DOS in Fig. 5(c) and 5(d) are the averages of 32 In atoms and 32 Sb atoms, respectively.

The total DOS in Figs. 4 and 5 show that the phase transition from crystal to liquid state results in the disappearance of the band gap around the Fermi level. That is, it changes the electronic states from those of a semiconductor to those of a metal. A study of the change of the partial DOS arising from the melting showed that the narrow s-bands at −9.5 and −5.5 eV in the crystalline state broaden without any significant changes in their peak positions and that the p-band states of both In and Sb drastically change so that their fine structures and band gap around the Fermi level disappear. These calculated results roughly agree with the GGA calculation reported in Ref. 19.

Figures 6 and 7 show the optical dielectric functions and refractive indices of InSb as a function of photon energy ($\hbar\,\omega$), respectively. Thin solid and dotted lines are the calculated results for crystal and liquid InSb, respectively. Open circles and the thick dashed line are the experimental data for crystal[32] and liquid[11] InSb, respectively. The calculated result for crystal InSb (thin solid lines) shows good agreement with experimental data (open circles). Especially, the three

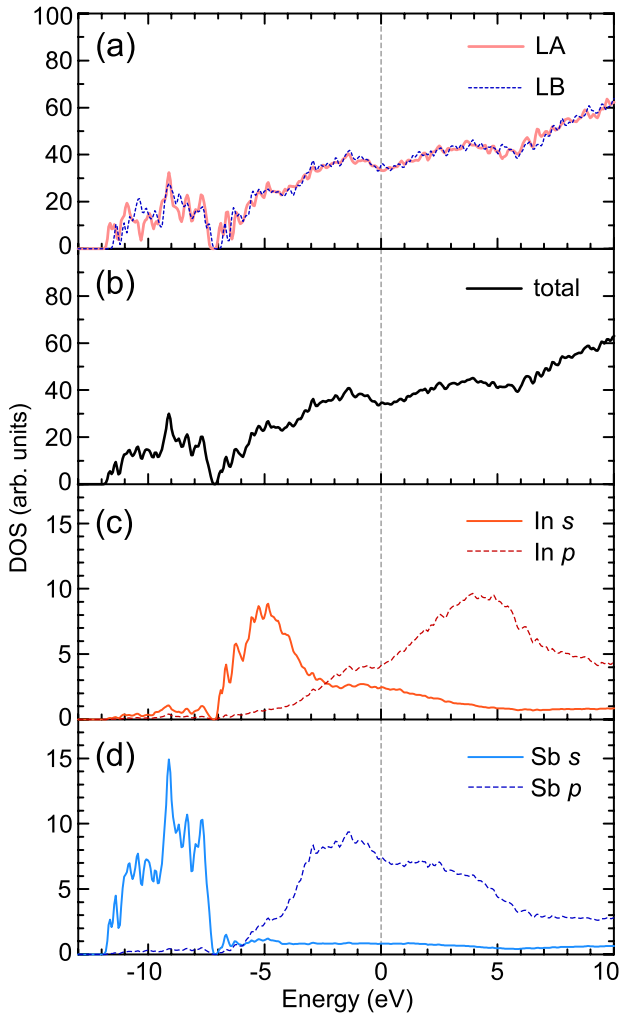

FIG. 5. Electronic density of states (DOS) of liquid InSb. (a) Total DOS of the LA and LB states. (b) Average of the total DOS of the LA and LB states. Partial DOS projected onto the molecular orbitals of In (c) and Sb (d).

peak positions corresponding to the critical point energies of E_1 = 1.9 eV, $E_1 + \Delta_1$ = 2.4 eV, and E_2 = 3.9 eV in the experimental data of Fig. 6(a) are well reproduced by the MBJLDA calculation. Note that the peak positions calculated by the GGA-PBE (thin dashed line) are shifted to lower energies by 0.3–0.5 eV. Similar shifts were also reported in previous studies performed using the LDA calculation.[13,14] Therefore, the MBJLDA calculation used here provides more accurate values for the excited electronic states of crystal InSb when compared with the GGA-PBE or LDA calculations.

During the phase transition from the crystal to liquid state, the optical response of InSb changes drastically. The experimental data for liquid InSb (thick dashed line in Figs. 6 and 7) show typical metallic properties, that is, as the photon energy decreases, the real and imaginary parts of the optical dielectric function divergently decreases and increases, respectively. Except for the real part of the optical dielectric function ($Re[\varepsilon]$), the calculated results for liquid InSb roughly agree with the experimental data. As shown in Fig. 6(b), the calculated $Re[\varepsilon]$ has a large deviation from the experimental data in the low energy region. In this study, the optical dielectric functions were calculated by considering only interband transitions. Therefore, the intraband contribution (Drude-like term), which increases with a decrease in photon energy, is proposed to be the reason for the deviation between the experimental data and the calculation.

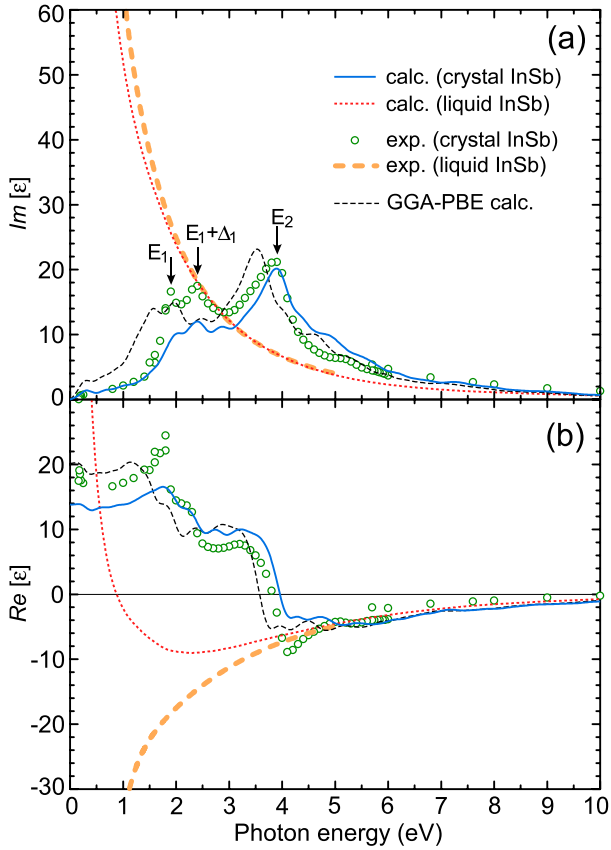

FIG. 6. (a) Imaginary and (b) real parts of the optical dielectric functions. The thin solid line and dotted line show the calculated dielectric functions of crystal and liquid InSb, respectively. Open circles and the thick dashed line are experimental data for crystal[32] and liquid[11] InSb, respectively. The thin dashed line shows the dielectric function of crystal InSb calculated by the GGA-PBE method.

Next, we shall focus on the imaginary part of the refractive index (k), because the value of k, representing the optical absorption, is important from the viewpoint of materials for the active layer in super-resolution optical discs. As shown in Fig. 7(a), in the photon energy range above 2 eV, the calculated result for k agrees with the experimental data within a margin of 15%. Therefore, our calculation can be used for a quantitative discussion. Table I shows the values of k at a photon energy of $\hbar\,\omega$ = 3.06 eV, corresponding to the wavelength of 405 nm, used in the Blu-ray Disc systems. The values in Table I show that k increases greatly because of the melting. We shall discuss the origin of this increase of k. As shown in Fig. 6(a), the imaginary part of the dielectric function ($Im[\varepsilon]$) at $\hbar\,\omega$ = 3.06 eV has similar values for both crystal and liquid states. This indicates that the oscillator strength of the optical transitions between the valence and conduction bands corresponding to $\hbar\,\omega$ = 3.06 eV does not change because of the melting. Thus, the increase of k does not originate from the optical transitions at $\hbar\,\omega$ =3.06 eV. If $Im[\varepsilon]$ does not change, the increase in k should result from the change in the sign of $Re[\varepsilon]$ from positive to negative, as derived from the following equation with the complex square root: $\tilde{n} = n + ik = \sqrt{\varepsilon}$. Indeed, as shown in Fig. 6(b), $Re[\varepsilon]$ at $\hbar\,\omega$ =3.06 eV greatly decreases from positive to negative values because of the melting. This means that the optical responses change to exhibit metallic behavior. According to the Drude–Lorentz model, the decrease in $Re[\varepsilon]$ at $\hbar\,\omega$ = 3.06 eV should arise from the increased optical transitions in the energy range lower than 3.06 eV. Because the DOS around the Fermi level grows because of the melting, as shown in Figs. 4 and 5, a very large increase of the optical transitions below 2 eV must occur. Therefore, it is suggested that the increase of the optical transitions below 2 eV provides the largest contribution to the increase of k at $\hbar\,\omega$ = 3.06 eV.

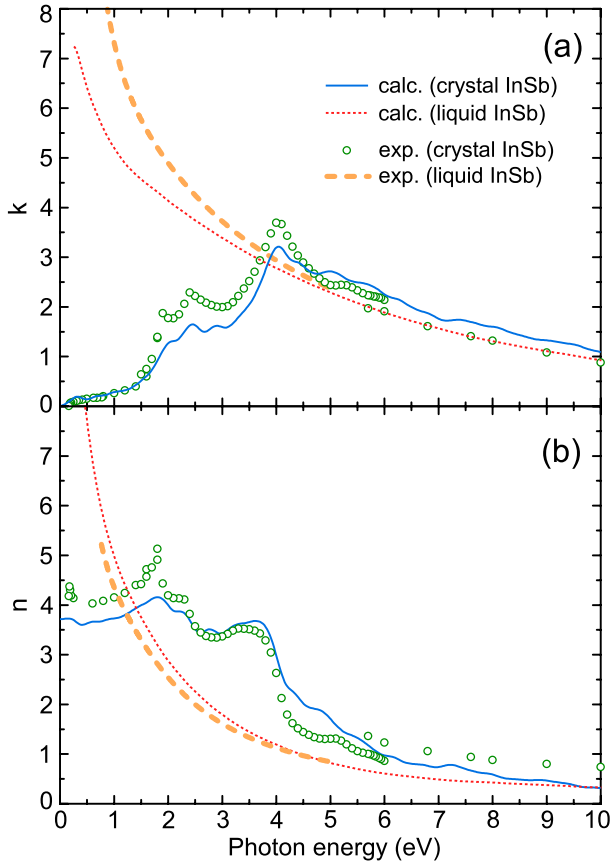

FIG. 7. (a) Imaginary and (b) real parts of the refractive indices. The thin solid line and dotted line show the calculated refractive indices of crystal and liquid InSb, respectively. Open circles and the thick dashed line are experimental data for crystal[32] and liquid[11] InSb, respectively.

TABLE I. Imaginary part of the refractive index at a photon energy of $\hbar\omega = 3.06$ eV.

	k (crystal InSb)	k (liquid InSb)	Δk
Experiment	2.01 [a]	3.67 [b]	1.66
Calculation (this study)	1.58	3.35	1.77

[a]Reference 32.
[b]Reference 11.

IV. CONCLUSION

We performed ab initio calculations on InSb to analyze the differences in the optical properties between the crystalline and liquid states. The calculated results indicate that the DOS around the Fermi level increases because of the phase transition from crystalline to liquid; and thus, the optical properties of InSb become metallic. We propose that the increase in the optical absorption at $\hbar\omega = 3.06$ eV arising from the melting originates from the increased optical transitions below 2 eV.

ACKNOWLEDGEMENTS

We thank Dr. M. Kuwahara for valuable discussions. This work was supported in part by the Japan Society for the Promotion of Science KAKENHI (Grants-in-Aid for Scientific Research) Grant Number 23560045, 15K04702.

[1] K. Yasuda, M. Ono, K. Aratani, A. Fukumoto, and M. Kaneko, Jpn. J. Appl. Phys. **32**, 5210 (1993).
[2] J. Tominaga, T. Nakano, and N. Atoda, Appl. Phys. Lett. **73**, 2078 (1998).
[3] T. Kikukawa, N. Fukuzawa, and T. Kobayashi, Jpn. J. Appl. Phys. **44**, 3596 (2005).
[4] J. Kim, I. Hwang, J. Bae, J. Lee, H. Park, I. Park, T. Kikukawa, N. Fukuzawa, T. Kobayashi, and J. Tominaga, Jpn. J. Appl Phys. **45**, 1370 (2006).
[5] M. Kuwahara, T. Shima, P. Fons, T. Fukaya, and J. Tominaga, J. Appl. Phys. **100**, 043106 (2006).
[6] K. Nakai, M. Ohmaki, N. Takeshita, B. Hyot, B. André, and L. Poupinet, Jpn. J. Appl. Phys. **49**, 08KE01 (2010).
[7] B. Hyot, Phys. Status Solidi B **249**, 1992 (2012).
[8] J. S. Kim, K. Kwak, and C. Y. You, Jpn. J. Appl. Phys. **47**, 5845 (2008).
[9] A. C. Assafrao, A. J. H. Wachters, S.F. Pereira, and H. P. Urbach, Jpn. J. Appl. Phys. **51**, 112501 (2012).
[10] H. Sano, T. Shima, M. Kuwahara, Y. Fujita, M. Uchiyama, and Y. Aono, J. Appl. Phys. **115**, 153104 (2014).
[11] M. Kuwahara, R. Endo, K. Tsutsumi, F. Morikasa, M. Suzuki, T. Shima, M. Susa, T. Endo, T. Tadokoro, and S. Hosaka, Appl. Phys. Express **6**, 082501 (2013).
[12] J. R. Chelikowsky and M. L. Cohen, Phys. Rev. B **14**, 556 (1976).
[13] M-Z. Huang and W. Y. Ching, Phys. Rev. B **47**, 9449 (1993).
[14] S. H. Rhim, M. Kim, A. J. Freeman, and R. Asahi, Phys. Rev. B **71**, 045202 (2005).
[15] Y-S. Kim, M. Marsman, G. Kresse, F. Tran, and P. Blaha, Phys. Rev. B **82**, 205212 (2010).
[16] J. H. Los, T. D. Kühne, S. Gabardi, and M. Bernasconi, Phys. Rev. B **87**, 184201 (2013).
[17] L. Wang, X. S. Chen, Y. Huang, W. Lu, and J. J. Zhao, Physica B **405**, 2481 (2010).
[18] L. Wang, X. Chen, W. Lu, and J. Zhao, Solid State Commun. **149**, 638 (2009).
[19] T. Gu, X. Bian, J. Qin, and C. Xu, Phys. Rev. B **71**, 104206 (2005).
[20] H. Sano and G. Mizutani, in *Proceedings of the 26th Symposium on Phase Change Oriented Science*, *Hamamatsu, Japan*, *4–5 December 2014*. edited by T. Saiki (2014), p. 69.
[21] G. Kresse and D. Joubert, Phys. Rev. B **59**, 1758 (1999).
[22] P. E. Blöchl, Phys. Rev. B **50**, 17953 (1994).
[23] G. Kresse and J. Furthmüller, Comput. Mater. Sci. **6**, 15 (1996).
[24] G. Kresse and J. Furthmüller, Phys. Rev. B **54**, 11169 (1996).
[25] J. P. Perdew, K. Burke, and M. Ernzerhof, Phys. Rev. Lett. **77**, 3865 (1996).
[26] F. Tran and P. Blaha, Phys. Rev. Lett. **102**, 226401 (2009).
[27] M. Gajdoš, K. Hummer, G. Kresse, J. Furthmüller, and F. Bechstedt, Phys. Rev. B **73**, 045112 (2006).
[28] *Landolt-Börnstein: Numerical Data and Functional Relationships in Science and Technology New Series Group III*, edited by O. Madelung, M. Schuz, and H. Weiss (Springer-Verlag, Berlin, 1982), Vol. 17a, p. 315.
[29] S. Nosé, J. Chem. Phys. **81**, 511 (1984).
[30] Y. Sato, T. Nishizuka, T. Takamizawa, T. Yamarura, and Y. Waseda, Int. J. Thermophys. **23**, 235 (2002).
[31] I. Vurgaftman, J. R. Meyer, and L. R. Ram-Mohan, J. Appl. Phys. **89**, 5815 (2001).
[32] R. T. Holm, in *Handbook of Optical Constants of Solids*, edited by E. D. Palik (Academic Press, New York, 1985), pp. 491-502.